Physica C 471 (2011) 889–892

Contents lists available at ScienceDirect

Physica C

journal homepage: www.elsevier.com/locate/physc

Simulation of flux dynamics in a superconducting bulk magnetized by multi-pulse technique

H. Fujishiro *, T. Naito, M. Oyama

Faculty of Engineering, Iwate University, 4-3-5 Ueda, Morioka 020-8551, Japan

ARTICLE INFO

Article history:
Available online 12 May 2011

Keywords:
Pulsed field magnetization
Simulation
Temperature rise
Flux intrusion
Bulk superconductor

ABSTRACT

We have simulated the time and spatial dependence of local field $B_z(t, r)$ and temperature $T(t, r)$ on the superconducting bulk during pulsed field magnetization (PFM) using the finite element method (FEM). A modified multi-pulse technique with step-wise cooling (MMPSC) was performed to the cryo-cooled bulk, which was experimentally confirmed to the effective PFM technique to enhance the trapped field B_z higher than 5 T. In the simulation, the B_z value at the center of the bulk surface was enhanced at the 2nd stage of the MMPSC method, in which the results of the simulation reproduced the experimental ones. The enhancement of B_z results from the reduction in the temperature because of the already trapped flux in the bulk at the 1st stage of the MMPSC method.

1. Introduction

REBaCuO superconducting bulk (RE: rare earth elements or Y) can trap a high magnetic field B_z using a pulsed field magnetization (PFM) as a substitute for field-cooled magnetization (FCM), which can be used for a magnetic separation, drag delivery system and so on. However, B_z by PFM is smaller than that by FCM because of a large heat generation due to the dynamical motion of magnetic flux in the bulk. To enhance B_z by PFM, a multi-magnetic pulse technique such as an iteratively magnetizing pulsed-field method with reducing amplitude (IMRA) [1] and a multi-pulse technique with step-wise cooling (MPSC) [2] is effective around 77 K. We have succeeded the highest field trap of 5.2 T on the GdBaCuO bulk 45 mm in diameter by a modified MPSC (MMPSC) at 29 K, which is a record-high value by PFM to date [3]. To explore the desired research direction to enhance the B_z value by PFM still more, it is necessary to analyze both the flux dynamics and the heat propagation theoretically.

Several theoretical studies for PFM have been reported in previous works [4,5]. We have also constructed the framework of theoretical simulation in the superconducting bulk and simulated the time and spatial dependence of local field $B_z(t, r)$ and temperature $T(t, r)$ in the superconducting bulk after a single magnetic pulse application, which reproduced the experimental results qualitatively [6]. However, the B_z value obtained by the simulation was smaller than the experimental ones. Recently, we have simulated the $B_z(t, r)$ and $T(t, r)$ for the successive pulsed field application with identical strength (SPA), and the enhancement of B_z was confirmed compared with a single pulse application [7]. Kajikawa et al. reported the enhancement of B_z by the MMPSC method using a simulation [8]. However, time evolution and position dependence of the magnetic field and temperature did not reported. As described in this paper, we performed the simulation to the MMPSC method for the higher J_c bulk, and investigated the flux dynamics and the temperature propagation during MMPSC.

2. Theoretical model and simulation

Based on our experimental setup around the bulk, the framework of the theoretical simulation was constructed. The detailed procedure of simulation and the used parameters were described elsewhere [6]. Commercial software, Photo-Eddy, combined with Photo-Thermo (Photon Ltd., Japan) was used for analysis of the magnetic field and temperature distribution in superconducting bulk during PFM. As shown in Fig. 1, a superconducting bulk disk 46 mm in diameter and 15 mm in thickness was stacked on the cold stage of the refrigerator in a vacuum chamber and cooled. The spacing plate with the thermal conductivity, k_{cont} (=0.5 W m^{-1} K^{-1}), between the bulk and the cold stage with 1 mm in thickness was set, which imaginarily represented both the cooling power of the refrigerator and the thermal contact of the bulk to the cold stage.

Physical phenomena during PFM are described by electromagnetic and thermal equations on the axisymmetric coordinate, which were referred from Ref. [9].

The power-n model ($n = 8$) was used to describe the nonlinear E–J characteristic in superconducting bulk as follows:

* Corresponding author. Tel./fax: +81 19 621 6363.
E-mail address: fujishiro@iwate-u.ac.jp (H. Fujishiro).

0921-4534/$ - see front matter © 2011 Elsevier B.V. All rights reserved.
doi:10.1016/j.physc.2011.05.081

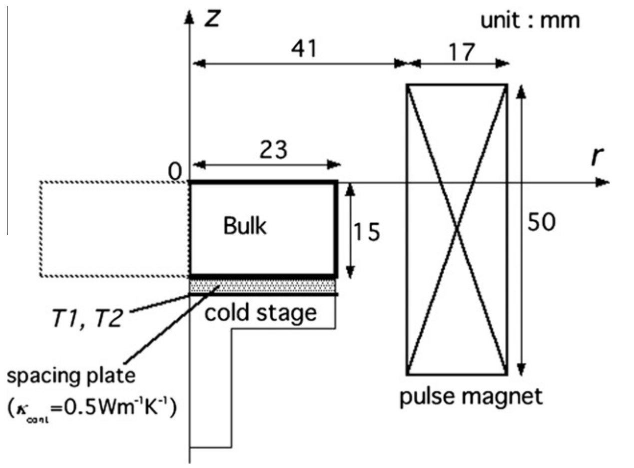

Fig. 1. Structure and dimensions around the superconducting bulk and solenoid copper coil for pulsed field magnetization (PFM).

$$E = E_c\left(\frac{J}{J_c}\right)^n, \tag{1}$$

where J_c is the critical current density and E_c (=1 × 10^{-6} V/m) is the reference electric field. The temperature and magnetic field dependence of $J_c(T, B)$ was described as

$$J_c(T,B) = \alpha\left\{1-\left(\frac{T}{T_c}\right)^2\right\}^{\frac{3}{2}}\frac{B_0}{|B|+B_0}, \tag{2}$$

where T_c (=92 K) is the critical temperature at B = 0, and B_0 (=1.3 T) is constant. The constant value of $\alpha = 1.83 \times 10^9$ A/m^2 was used in this study, which showed J_c (40 K, 0 T) = 1.33 × 10^9 A/m^2 and was a typical value of the superconducting bulk at present [10]. Iterative calculation was performed to obtain the convergence of electrical conductivity σ in the bulk at each time step. The pulsed field $B_{ex}(t)$ with a rise time of τ = 0.013 s and with a pulse duration of 0.13 s was applied using a solenoid pulsed coil.

The sequence of the MMPSC technique was shown in the inset of Fig. 2a [3]. Four magnetic pulses were applied at different initial temperatures $T1$ and $T2$ to the bulk. In the simulation, at the 1st stage in the MMPSC, a pulse field of $B1$ was applied twice (No. 1 and No. 2 pulses) at $T1$ in order to trap a small number of magnetic fluxes with concave B_z profile on the bulk surface. At the 2nd stage, the bulk was cooled down to $T2$ (<$T1$) and a higher pulse field of $B2$ (>$B1$) was applied twice (No. 3 and No. 4 pulses).

3. Experimental results

First we show an example of the experimental results of the flux dynamics in the bulk magnetized by the MMPSC method [3]. Fig. 2a and b shows respectively the ascending ($t \leqslant 0.013$ s) and descending ($t \geqslant 0.013$ s) stages of the local field $B_z(r, t)$ on the surface of the GdBaCuO bulk (45 mm in diameter and 18 mm in thickness) after applying the No. 1 pulse ($B1$ = 4.5 T at $T1$ = 45 K). The $B_z(t)$ values at positions C (r = 0), M (r = 8 mm) and E (r = 15 mm) were measured by three Hall sensors adhered on the bulk surface. For the ascending process, the flux intrusion starts to increase from the bulk periphery and the small amount of the magnetic flux arrives at the bulk center. For the descending process, the intruded flux gradually escaped in the region outer than r = 8 mm and the "*M-shaped*" profile can be obtained.

Fig. 3a and b shows the $B_z(r, t)$ profiles for the No. 3 pulse ($T2$ = 29 K, $B2$ = 6.7 T) at the 2nd stage of the MMPSC. $B_z(t)$ at the position E increases, but $B_z(t)$ at the position C and $B_z(t)$ at the position M hardly change for the ascending process. For the descending process, however, $B_z(t)$ at the position C sharply increased at t = 0.013 s, $B_z(t)$ at the position M also slightly increased and the conical trapped field distribution was realized. These behaviors suggest that the already trapped flux at the 1st stage was pushed into the bulk center and that the additional flux was supplied from the peripheral region. As a result, the highest B_z was trapped at the bulk center by the MMPSC method. The temperature rise at the 2nd stage was decreased experimentally, compared with that after a single pulse application with the same amplitude to the virgin state bulk because of the already trapped flux at the 1st stage [3].

4. Results of simulation and discussion

Fig. 4a shows the results of the simulation of the trapped field profile $B_z(r)$ on the bulk surface at T = 60 K as a function of applied pulsed field. $B_z(r)$ profile changes from the "*M-shaped*" profile to the convex-shaped one with increasing applied field. We adopted B = 6.5 T as the applied field of $B1$ for the 1st stage in the MMPSC method. Because the "*M-shaped*" profile at the 1st stage is necessary to enhance B_z at the 2nd stage. Fig. 4b shows the trapped field

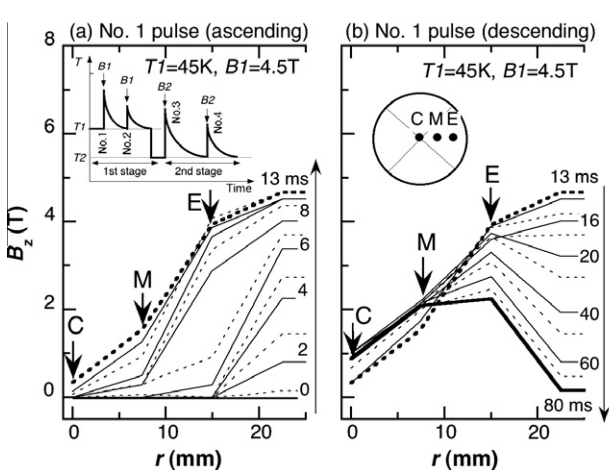

Fig. 2. Examples of experimental results for the time evolution of the local field $B_z(t)$ as a function of the distance along the r-direction for the No. 1 pulse ($T1$ = 45 K, $B1$ = 4.5 T) of (a) ascending ($t \leqslant 0.013$ s) and (b) descending ($t \geqslant 0.013$ s) stages in MMPSC, respectively [3].

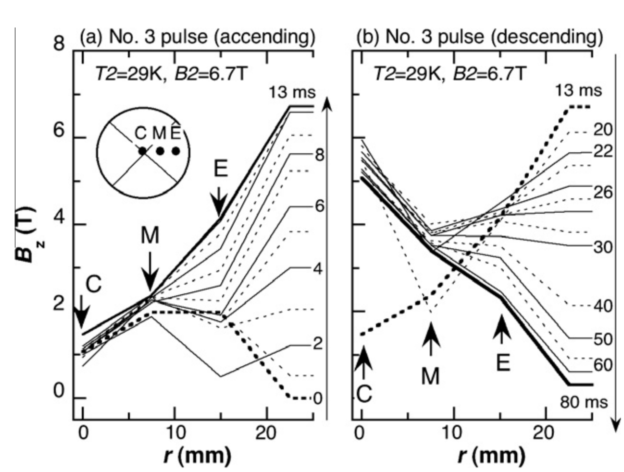

Fig. 3. Examples of experimental results for the time evolution of the local field $B_z(t)$ as a function of the distance along the r-direction for the No. 3 pulse ($T2$ = 29 K, $B2$ = 6.7 T) of (a) ascending ($t \leqslant 0.013$ s) and (b) descending ($t \geqslant 0.013$ s) stages in MMPSC, respectively [3].

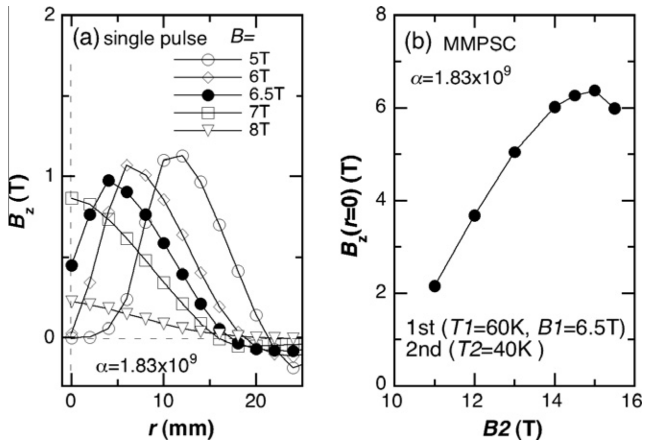

Fig. 4. (a) The results of the simulation of the trapped field profile $B_z(r)$ on the bulk surface at 60 K as a function of applied pulsed field. (b) The trapped field $B_z(r = 0)$ after the termination of MMPSC method as a function of the applied field $B2$ at the 2nd stage at $T2$ = 40 K.

$B_z(r = 0)$ after the termination of the MMPSC method as a function of the applied field $B2$ at the 2nd stage at $T2$ = 40 K. The final trapped field increases with increasing $B2$ and takes a maximum of 6.2 T at $B2$ = 15 T, which suggests that an optimum $B2$ exists for each condition of $T1$, $T2$ and $B1$.

Fig. 5a and b shows the pulse number dependence of the trapped field profile $B_z(r)$ on the bulk surface for $B2$ = 11 T and 15 T at $T2$ = 40 K, respectively. For $B2$ = 11 T, the magnetic flux did not sufficiently reach the bulk center and the $B_z(r)$ profile is still concave. On the other hand, for $B2$ = 15 T, the $B_z(r)$ profile changed to cone-shaped one and the maximum $B_z(r = 0)$ = 6.1 T was obtained for the No. 4 pulse. In the multi-pulse magnetization process, already trapped flux was treated as the shielding current in the bulk in the simulation and the additional magnetic flux was superposed.

Fig. 6a and b, respectively, present the time evolution and spatial distribution of the local magnetic field $B_z(t, r)$ and the temperature $T(t, r)$ on the bulk surface after applying a No. 1 pulse of $B1$ = 6.5 T at $T1$ = 60 K in MMPSC. The left and right parts for each figure are for the ascending ($t \leqslant 0.013$ s) and descending ($t \geqslant 0.013$ s) stages, respectively. In Fig. 6a, the magnetic flux intrudes gradually into the bulk from the bulk periphery. For the descending stage, the magnetic field decreased gradually at the outer region with increasing time. The local field near $r = 0$ remains to zero at $t = 0.1$ s and then increases gradually to $B_z = 0.5$ T at the steady state. As a result, the concave shaped profile was realized. The results of the simulation reproduce the experimental ones qualitatively as shown in Figs. 2 and 3.

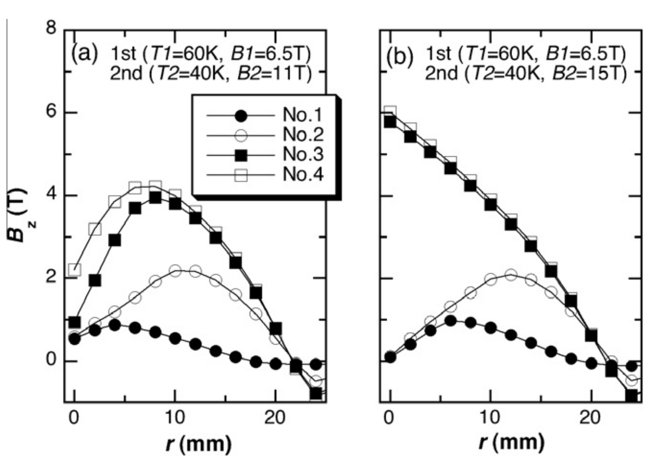

Fig. 5. The pulse number dependence of the trapped field profile $B_z(r)$ on the bulk surface for (a) $B2$ = 11 T and (b) $B2$ = 15 T at $T2$ = 40 K.

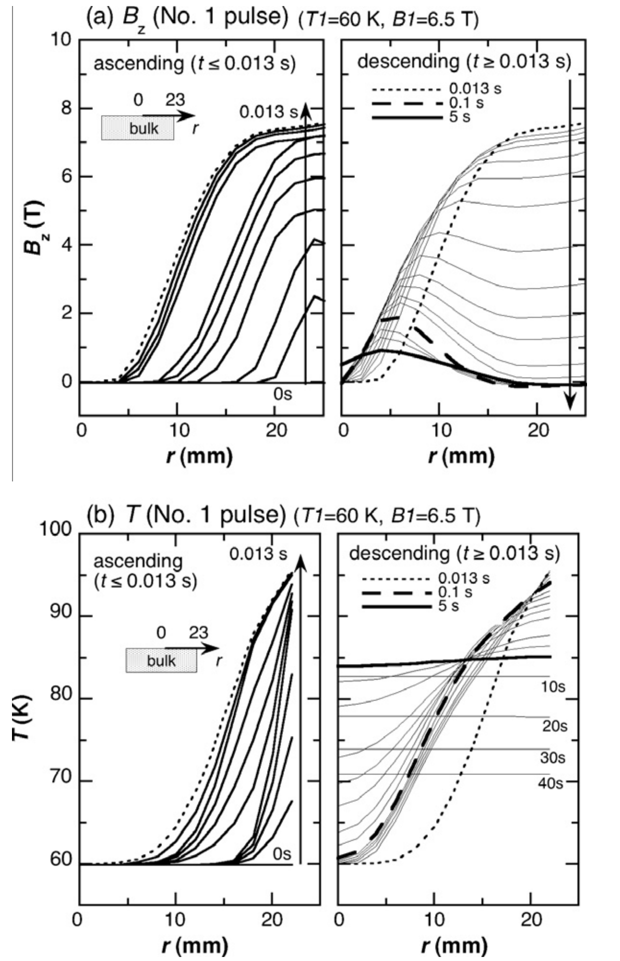

Fig. 6. The time evolution and spatial distribution of the (a) local magnetic field $B_z(t, r)$ and (b) temperature $T(t, r)$ on the bulk surface after applying No. 1 pulse of $B1$ = 6.5 T at $T1$ = 60 K in MMPSC.

In Fig. 6b, the temperature $T(t)$ at the bulk periphery gradually increased with time at the ascending stage, e.g., T = 95 K at t = 0.013 s. However, $T(t)$ at $r = 0$ remained to 40 K. At the descending stage, the generated heat diffuses to the bulk center gradually. After an isothermal temperature profile took place along the r-direction around t = 5 s, $T(t)$ decreased with increasing time. In this case, temperature gradient existed along the z-direction because the bottom of the bulk was fixed at 60 K.

Fig. 7a and b depict $B_z(t, r)$ and $T(t, r)$ on the bulk surface after applying No. 3 pulse of $B2$ = 15 T at the 2nd stage in MMPSC ($T2$ = 40 K). For the ascending stage, the magnetic flux intrudes gradually into the bulk from the bulk periphery and $B_z(r = 0)$ reached 2.3 T at t = 0.013 s. For the descending stage, $B_z(r = 0)$ increased to 7 T at t = 0.1 s and then decreased gradually to B_z = 6 T at t = 5 s. In Fig. 7b, the $T(t, r)$ behavior is the similar time and radius dependences to that for the No. 1 pulse, but the temperature rise is fairly reduced; T_{max} = 56 K at t = 7 s.

Fig. 8a and b respectively show the time dependence of the local field $B_z(t)$ and the temperature $T(t)$ at the center of the bulk surface ($r = 0$) for the MMPSC method, which were re-plotted from Figs. 6 and 7. The normalized applied pulsed field $B_{ex}(t)$ is also described to the right ordinates in Fig. 8a. $B_z(t)$ for the No. 1 pulse increases slightly to 0.7 T with time and that for the No. 2 pulse hardly

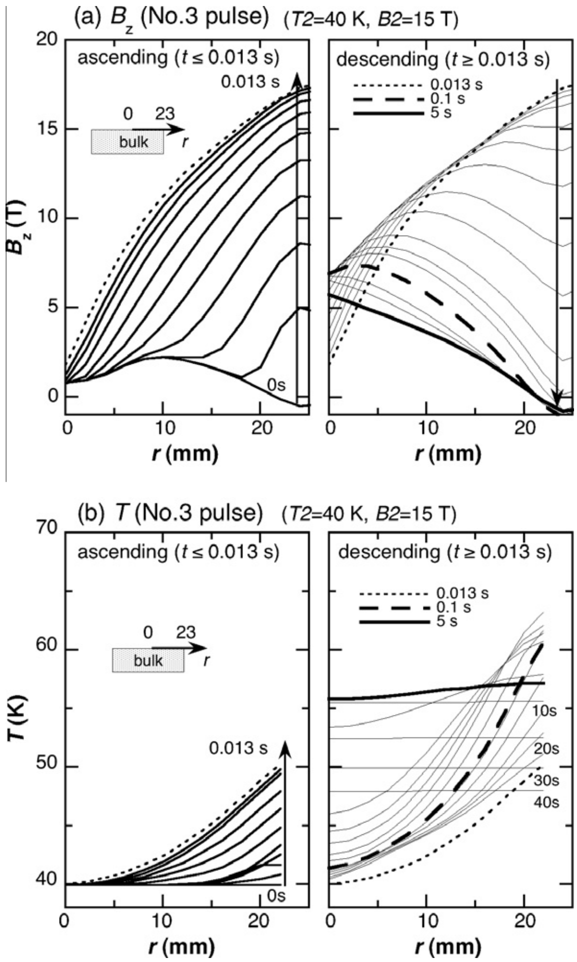

Fig. 7. The time evolution and spatial distribution of the (a) local magnetic field $B_z(t, r)$ and (b) temperature $T(t, r)$ on the bulk surface after applying No. 3 pulse of $B2$ = 15 T at the 2nd stage in MMPSC ($T2$ = 40 K).

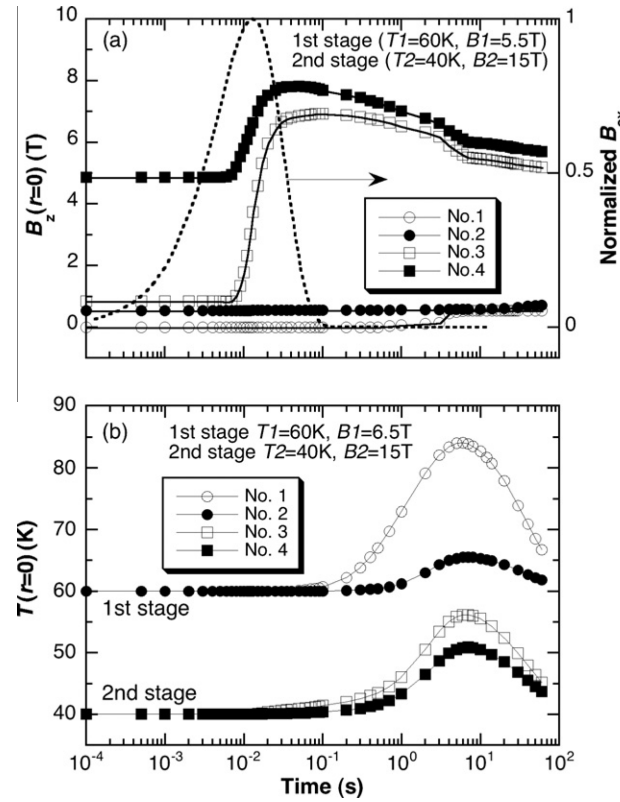

Fig. 8. The time dependence of the local field $B_z(t)$ and the temperature $T(t)$ at the center of the bulk surface (r = 0) for the MMPSC method, which were re-plotted from Figs. 6 and 7. The normalized applied pulsed field $B_{ex}(t)$ is also described by a dotted line in (a).

increases. On the other hand, for the No. 3 pulse at the 2nd stage, $B_z(t)$ starts to rise around t = 0.1 s, takes a maximum of 7 T, and approaches gradually to the final value. For the No. 4 pulse, the similar time dependence of the local field can be seen and the final value increased slightly. In Fig. 8b, at the 1st stage ($T1$ = 60 K), the simulated $T(t)$ for the No. 1 pulse takes a maximum of 85 K at t = 7 s and then decreases with increasing time. The maximum temperature T_{max} drastically decreases to 65 K for the No. 2 pulse. The time, at which $T(t)$ takes a maximum, is decided by the thermal conductivities of the bulk (k_{ab}, k_c) and the cooling power, and the time is independent of the pulse number. For the 2nd stage ($T2$ = 40 K), $T(t)$ for the No. 3 pulse takes a maximum of 57 K at t = 7 s and then decreases with increasing time. T_{max} drastically decreases to 51 K for the No. 4 pulse.

In the simulation above mentioned, the optimum parameters, $T1$ = 60 K, $B1$ = 6.5 T, $T2$ = 40 K and $B2$ = 15 T, were decided, which were different with those experimentally obtained; $T1$ = 45 K, $B1$ = 4.5 T, $T2$ = 29 K and $B2$ = 6.7 T. The essence of the MMPSC method is that the lower magnetic pulse $B1$ is applied twice at higher temperature $T1$ to realize the "*M-shaped*" profile at the 1st stage, and the higher and optimum magnetic pulse of $B2$ is applied twice at lower temperature $T2$ at the 2nd stage. Experimentally, the optimum parameters depend strongly on the characteristics of the bulk such as the magnitude and distribution of J_c. Taking these facts into consideration, the results of the simulation shown in this paper reproduce the experimental ones qualitatively.

In summary, we have simulated the time and spatial dependence of local field $B_z(t, r)$ and temperature $T(t, r)$ on the cryo-cooled superconducting bulk during a modified multi-pulse technique with step-wise cooling (MMPSC). In the simulation, the B_z value was enhanced at the 2nd stage in the MMPSC method, which reproduced the experimental results qualitatively. The enhancement of B_z at the 2nd stage results from the reduction in the temperature because of the already trapped flux in the bulk at the 1st stage in MMPSC.

References

[1] Y. Yanagi, Y. Itoh, M. Yoshikawa, T. Oka, T. Hosokawa, H. Ishihara, H. Ikuta, U. Mizutani, Adv. Supercond. XII, Springer-Verlag, Tokyo, 2000. p. 470.
[2] M. Sander, U. Sutter, R. Koch, M. Klaser, Supercond. Sci. Technol. 13 (2000) 841.
[3] H. Fujishiro, T. Tateiwa, A. Fujiwara, T. Oka, H. Hayashi, Physica C 445–448 (2006) 334.
[4] H. Ohsaki, T. Shimosaki, N. Nozawa, Supercond. Sci. Technol. 15 (2002) 754.
[5] Z. Xu, R. Lewin, A.M. Campbell, D.A. Cardwell, H. Jones, J. Phys. Conf. Ser. 234 (2010) 012049.
[6] H. Fujishiro, T. Naito, Supercond. Sci. Technol. 23 (2010) 105021.
[7] H. Fujishiro, T. Naito, D. Furuta, IEEE Appl. Supercond. in press.
[8] K. Kajikawa, R. Yokoo, K. Tomachi, K. Enpuku, K. Funaki, H. Hayashi, H. Fujishiro, Physica C 468 (2008) 1494.
[9] Y. Komi, M. Sekino, H. Ohsaki, Physica C 469 (2009) 1262.
[10] Y. Ishii, J. Shimoyama, H. Ogino, K. Kishio, J. Cryog. Soc. Jpn. 44 (2009) 573.